Front. Med. 2023, 17(2): 290−303
https://doi.org/10.1007/s11684-022-0956-8

RESEARCH ARTICLE

Repurposed benzydamine targeting CDK2 suppresses the growth of esophageal squamous cell carcinoma

Yubing Zhou[1,2,*], Xinyu He[1,2,*], Yanan Jiang[1,2,3,4,*], Zitong Wang[1], Yin Yu[1,2], Wenjie Wu[1,2], Chenyang Zhang[1], Jincheng Li[1], Yaping Guo[1,3], Xinhuan Chen[1,3], Zhicai Liu[4,6], Jimin Zhao[1,3,4,5], Kangdong Liu (✉)[1,2,3,4,5], Zigang Dong (✉)[1,2,3,5]

[1]*The Pathophysiology Department, School of Basic Medical Sciences, Academy of Medical Sciences, Zhengzhou University, Zhengzhou 450000, China;* [2]*The China-US (Henan) Hormel Cancer Institute, Zhengzhou 450000, China;* [3]*State Key Laboratory of Esophageal Cancer Prevention and Treatment, Zhengzhou 450000, China;* [4]*Provincial Cooperative Innovation Center for Cancer Chemoprevention, Zhengzhou University, Zhengzhou 450000, China;* [5]*Cancer Chemoprevention International Collaboration Laboratory, Zhengzhou 450000, China;* [6]*Oncology Department, The Tumor Hospital of Linzhou City, Linzhou 456500, China*

Abstract **Esophageal squamous cell carcinoma (ESCC) is one of the leading causes of cancer death worldwide. It is urgent to develop new drugs to improve the prognosis of ESCC patients. Here, we found benzydamine, a locally acting non-steroidal anti-inflammatory drug, had potent cytotoxic effect on ESCC cells. Benzydamine could suppress ESCC proliferation *in vivo* and *in vitro*. In terms of mechanism, CDK2 was identified as a target of benzydamine by molecular docking, pull-down assay and *in vitro* kinase assay. Specifically, benzydamine inhibited the growth of ESCC cells by inhibiting CDK2 activity and affecting downstream phosphorylation of MCM2, c-Myc and Rb, resulting in cell cycle arrest. Our study illustrates that benzydamine inhibits the growth of ESCC cells by downregulating the CDK2 pathway.**

Keywords benzydamine; cyclin-dependent kinase 2; patient-derived xenograft; esophageal squamous cell carcinoma

Introduction

Esophageal cancer (EC) is histopathologically classified into esophageal squamous cell carcinoma (ESCC) and esophageal adenocarcinoma (EAC) [1]. ESCC accounts for over 90% of diagnosed EC each year [2]. Currently, a combination therapy of surgical resection, radiotherapy, and chemotherapy is the primary approach for EC treatment. However, the overall five-year survival rate for advanced ESCC remains lower than 15%, and the recurrence rate is still high [3–5]. Therefore, it is essential to identify effective drugs for ESCC treatment or chemoprevention.

Chemoprevention is a new strategy used to slow the onset of cancers and reduce the relapse after primary treatment [6,7]. Over the past few years, many drugs approved by the United States Food and Drug Administration (FDA) are being used as chemopreventive agents owing to their safety and pharmacodynamic characteristics [8]. Several non-steroidal anti-inflammatory drugs (NSAIDs) such as aspirin and ibuprofen have been widely reported in cancer chemoprevention. By screening FDA-approved drugs, we found that benzydamine, a NSAID, could suppress the proliferation of ESCC cells. Benzydamine has been shown to possess local anesthetic and analgesic properties [9]. However, its anti-tumor activity and underlying molecular mechanisms have not been elucidated.

Cyclin-dependent kinase 2 (CDK2) is a vital kinase in cell cycle regulation and involved in a series of biological processes [10,11]. CDK2 plays an important role in cancer cell proliferation and correlates with cancer patients' survival [12,13]. Additionally, emerging evidence has demonstrated that inhibition of CDK2 elicits an anti-tumor activity in a subset of tumors [14]. Therefore, CDK2-selective inhibitors might present a therapeutic opportunity for CDK2 highly expressed cancers [15]. In this study, we elucidated the anti-tumor effect of benzydamine in ESCC *in vitro* and *in vivo*, which was

Received December 7, 2021; accepted August 18, 2022
Correspondence: Kangdong Liu, kdliu@zzu.edu.cn;
Zigang Dong, dongzg@zzu.edu.cn

*These authors contributed equally to this work.

shown to be achieved through the attenuation of the CDK2 related signaling pathways. Our results suggested that benzydamine suppressed ESCC growth by targeting CDK2.

Material and methods

Reagents and antibodies

Benzydamine (CAS: 642-72-8, # B414053) was purchased from J&K Scientific (Beijing, China) for the study. Sepharose 4B beads were purchased from GE Healthcare (Piscataway, NJ, USA). Fetal bovine serum (FBS), Roswell Park Memorial Institute (RPMI) 1640 medium, and Dulbecco's Modified Eagle's medium (DMEM) were purchased from Biological Industries (Beit HaEmek, Israel). Antibodies against MCM2 Ser41 (#ab109270), MCM2 (#ab108935), Rb Thr826 (#ab133446), and Rb (#ab181616) were purchased from Abcam (Cambridge, England). Antibodies against c-Myc Ser62 (#13748) and c-Myc (#9402) were purchased from Cell Signaling Technology (Danvers, MA, USA). The antibody against glyceraldehyde 3-phosphate dehydrogenase (GAPDH) (60004-1-Ig) was purchased from Proteintech Group (Wuhan, China).

Cell culture and cell lines

Human immortalized cell line Shantou human embryonic esophageal (SHEE) cells were obtained from Professor Enmin Li of Shantou University (Shantou, China). The ESCC cell lines (KYSE70, KYES140, KYSE150, KYSE410, KYSE450, KYSE510) were purchased from the Chinese Academy of Sciences Cell Bank (Shanghai, China). KYSE150 cells were cultured in RPMI 1640 medium containing 10% FBS, 0.1% penicillin (North China Pharmaceutical Group Corp, Shijiazhuang, China), and 0.1% streptomycin (Shandong Lukang Pharmaceutical Group, China). KYSE450 cells were cultured in DMEM containing 10% FBS, 0.1% penicillin, and 0.1% streptomycin. All these cell lines were incubated at 37 °C and an atmosphere of 5% CO_2 in a sterile incubator.

Cell proliferation assay

SHEE (2×10^3 cells/well), KYSE150 (3×10^3 cells/well), and KYSE450 (5×10^3 cells/well) cells were seeded in 96-well plates and cultured for 16–18 h. The cells were treated with different concentrations of benzydamine (0, 2.5, 5, 10, or 20 μM). Nuclei were stained using 4′, 6-diamidino-2-phenylindole (DAPI), and the cells were counted at various time points (0, 24, 48, 72, and 96 h) using IN Cell Analyzer 6000.

Anchorage-independent cell growth assay

KYSE150 and KYSE450 cells (8×10^3 cells/well) were suspended in RPMI 1640 and DMEM containing 0.3% agar and 10% FBS at various concentrations of benzydamine (0, 2.5, 5, 10, or 20 μM). Cells were cultured at 37 °C in 5% CO_2 for 10 days. Colonies were measured and analyzed using the IN Cell Analyzer 6000 software.

Plate cloning assay

KYSE150 and KYSE450 cells (3×10^2 cells/well) were seeded in 6-well plates and treated with various doses of benzydamine (0, 2.5, 5, 10, or 20 μM) for 10 days. Crystal violet (0.3%; Solarbio, Beijing, China) was used for staining clones for 4 min. Colonies were counted and photographed.

Cell sample preparation and phosphoproteomics analysis

KYSE150 cells (4.5×10^6) were seeded in 15 cm dishes. After 20 μM benzydamine treatment for 24 h, cells were lysed in lysis buffer (RIPA lysate, Solarbio, Beijing, China, #R0020). The lysates were then centrifuged the samples to remove the debris, and the supernatant was collected. The samples were digested with trypsin and the tryptic peptides were fractionated via high pH reverse-phase HPLC by a Thermo Betasil C18 column (5 μm particles, 10 mm ID, 250 mm length). In brief, peptides were separated with a gradient of 8%–32% acetonitrile (pH = 9.0) for approximately 60 min, resulting in 60 fractions. Subsequently, peptides were combined into six fractions and dried by vacuum centrifugation. Peptides were first subjected to a nanospray ionization source and then tandem mass spectrometry (MS/MS) in a Q ExactiveTM Plus (Thermo Fisher Scientific, Waltham, MA, USA) coupled online to the UPLC. Data were obtained by searching through UniProt for identified peptides assembled as proteins. The resulting MS/MS data were processed using the MaxQuant search engine (v.1.5.2.8) and analyzed.

Western blotting

Proteins were extracted using RIPA lysis buffer (Solarbio, Beijing, China, #R0020) and quantified using a bicinchoninic acid (BCA) assay kit (#P0011-1, #P0011-2, Beyotime, Shanghai, China). Equal amounts of protein were prepared according to protein concentration and separated by SDS-PAGE. Proteins were subsequently electrophoretically transferred onto polyvinylidene fluoride membranes. After blocking with 5% bovine

serum albumin (#A8020, Solarbio, Beijing) or skimmed milk for 60 min at 25 °C, membranes were incubated with specific primary antibodies at 4 °C. Subsequently, incubation with horseradish peroxidase (HRP)-conjugated secondary antibodies was performed for 2 h at 25 °C. Bands were visualized by the enhanced chemiluminescence detection reagent (GE Healthcare, Little Chalfont, UK). Primary antibodies were used: anti-p-MCM2 Ser41 (#ab109270, 1:50000, Abcam, Cambridge, England), anti-MCM2 (#ab108935, 1:1000, rabbit monoclonal, Abcam, Cambridge, England), anti-p-Rb (Thr826) (#ab133446, 1:1000, rabbit monoclonal, Abcam, Cambridge, England), anti-Rb (#ab181616, 1:2000, rabbit monoclonal, Abcam, Cambridge, England), anti-p-c-Myc (Ser62) (#13748, 1:1000, rabbit monoclonal, Cell Signaling Technology, Danvers, MA, USA), anti-c-Myc (#9402, 1:1000, Polyclonal rabbit, Cell Signaling Technology, Danvers, MA, USA), and GAPDH (60004-1-Ig, 1:20,000, mouse monoclonal, Proteintech Group, Wuhan, China).

Cell cycle analysis

The 3×10^5 cells were seeded in 60 mm plates and synchronized by serum starvation for 24 h. Cells were then treated with benzydamine (0, 2.5, 5, 10, or 20 μM) for 24 or 48 h in 10% serum-supplemented medium. For cell cycle analysis, cells were harvested and washed twice with phosphate buffered saline, fixed in 70% ethanol (Tianjin Zhiyuan Chemical Reagent Co., Ltd, Tianjin, China), and stored at −20 °C for 24 h. Cells were stained with propidium iodide (Beyotime, Shanghai, China) for cell cycle assessment, followed by analysis using a FACS Calibur Flow Cytometer (BD Biosciences, San Jose, CA, USA).

Kinase prediction, target prediction, and correlation analysis

Kinase prediction of benzydamine was carried out via iGPS1.0. Swiss TargetPrediction [16] and SwissDock [17] were used to predict the targets of benzydamine. Correlation analysis of CDK2 and MCM2 was performed using The Cancer Genome Atlas (TCGA) database [18].

Molecular docking of CDK2 with benzydamine

To explore the interaction between CDK2 and benzydamine, we performed *in silico* docking using the autodock software programs. First, the crystal structure of CDK2 was downloaded from the Protein Data Bank (PDB) (ID: 1AQ1) and CDK2 was prepared using standard procedures of the Protein Preparation Wizard (autodock). Hydrogen atoms were added at a pH of 7.0, and all water molecules were removed. The drug benzydamine was prepared for docking by using the default parameters in the LigPrep program. Subsequently, the docking of benzydamine to CDK2 was achieved using default parameters in the extra precision mode in the Glide program.

Pull-down assay using Sepharose 4B beads

Benzydamine-Sepharose 4B beads and dimethyl sulfoxide (DMSO)-Sepharose 4B beads were prepared according to the manufacturer's instructions [19]. Cell lysates (500 μg), active CDK2 (200 ng), and 293F cell lysate (500 μg) were incubated with benzydamine-Sepharose 4B beads and DMSO-Sepharose 4B beads in 1× reaction buffer (50 mM Tris pH 7.5, 5 mM EDTA, 150 mM NaCl, 1 mM DTT, 0.01% NP-40, 2 μg/mL bovine serum albumin) at 4°C with gentle rotation overnight. Beads were washed thrice with washing buffer (50 mM Tris-HCl pH 7.5, 5 mM EDTA, 150 mM NaCl, 1 mM DTT, 0.2 mM PMSF, and 0.01% NP-40) after incubation. CDK2 bands were analyzed by Western blotting.

Protein purification

PET-28a-CDK2 and MCM2 plasmids (YouBio Biotechnology Company, Hunan, China) were transformed into *E. coli* and amplified. Following amplification, the cells were lysed with ultrasounds, and the proteins were purified by nickel column. CDK2 and MCM2 proteins were identified via Western blotting and Coomassie blue staining.

***In vitro* kinase assay**

In vitro kinase assay was performed using an assay kit according to the manufacturer's instructions. Human recombined MCM2 protein (1 μg), as a substrate for CDK2, was mixed with active CDK2 (500 ng) and different doses of benzydamine in a 25 μL reaction mixture, then was supplemented with 20 μM ATP and 1× kinase buffer (Cell Signaling Technology, Danvers, MA, USA) and incubated at 30 °C for 30 min. Reactions were blocked by the addition of 5 μL 6× loading buffer, and proteins were analyzed by Western blotting.

Lentivirus production and infection

KYSE150 and KYSE450 cells were transfected with short hairpin RNA (shCDK2). The shCDK2 plasmids were cloned into the pLKO.1 lentiviral expression vector. The CDK2 clones (#1F: 5′-CCTCAGAATCTGCTTATT AAC-3′; #2F: 5′-GCCCTCTGAACTTGCCTTAAA-3′) were purchased from Sangon Biotech (Shanghai, China). Both the viral and packaging vectors were transfered to

HEK293T cells (60%–80% confluence). After 4 h, cells were replaced with fresh medium (DMEM). The lentiviral particles were harvested at 24, 48, and 72 h by filtration using a 0.22 μm filter. KYSE150 and KYSE450 cells (60% confluence) were infected with medium containing lentiviral particles and 8 μg/mL polybrene for 12 h. Cells were then re-incubated in fresh medium for 24 h. Subsequently, 1 μg/mL (KYSE450) or 2 μg/mL (KYSE150) puromycin was used for cell selection. The transfection efficiencies were analyzed by Western blotting. The cell proliferation and colony formation ability of knockdown cells was examined in comparison with mock-transfected cells. KYSE450 and KYSE150 cells were transfected with shCDK2 in a similar manner.

Patient-derived xenograft (PDX) mouse model

All the protocols used in this study were approved by the Research Ethics Committee of Zhengzhou University (Zhengzhou, China). ESCC tissues were obtained from the Linzhou Tumour Hospital (Linzhou, China). The protocols for establishing PDX models have been previously described [20,21]. Female, severe combined immunodeficient (SCID) mice (age, 6–8 weeks) were used for these experiments. Tumor tissues from patients were subcutaneously implanted into the back of SCID mice. When the tumor volume reached about 100 mm^3, mice were randomly divided into three treatment groups (8/group) as follows: (1) vehicle; (2) 5 mg/kg benzydamine; (3) 50 mg/kg benzydamine. Benzydamine was administered once a day by oral gavage for about 30 days. Bodyweights were monitored three times a week. The tumor volume was measured twice a week. Tumor volumes were calculated using the following formula: $V = LD \times (SD)^2/2$, where V is tumor volume. When the average tumor volume reached 1000 mm^3, the mice were euthanized under anesthesia and tumors were extracted.

Immunohistochemistry

Formalin-fixed tumor tissues were cut into 4 μm sections, then deparaffinized and hydrated for immunohistochemistry. Samples were baked in a constant-temperature oven at 65°C, and citrate acid was used for antigen retrieval. All the tissue sections were blocked with 3% H_2O_2 for 10 min in the dark. Sections were then hybridized with specific antibodies (Ki-67, 1:50, MCM2 S41, 1:200; Abcam) for 16 h at 4°C and then incubated with HRP-conjugated goat anti-rabbit or mouse IgG antibody (ZSGB-BIO, Beijing, China) for 30 min. After DAB staining for 2 min, sections were counterstained with hematoxylin (Baso, Zhuhai, China) for 1 min, dehydrated in a graded series of alcohol to xylene, and covered with glass coverslips. All sections were observed under a microscope and scanned by the TissueFaxes (version 4.2). Image-Pro Plus software (version 6) was used for evaluating the positive cells.

Statistical analysis

One-way analysis of variance or Student's *t*-test was used to compare significant differences; $P < 0.05$ was considered significant. All quantitative results have been expressed as mean ± standard deviation or standard error as indicated.

Results

Benzydamine suppressed anchorage-dependent and -independent growth of ESCC

To identify a novel drug against ESCC, we screened FDA-approved drugs by performing a cytotoxic assay on KYSE450 cells. Benzydamine, a NSAID, exhibited significant cytotoxic effects to KYSE450 cells (Fig. 1A and 1B). To test the cytotoxic effect of benzydamine on ESCC, we treated several different ESCC cell lines (KYSE70, KYES140, KYSE150, KYSE410, KYSE450, KYSE510) and SHEE with different concentrations of benzydamine for 24 and 48 h. Our results indicated that the half maximal inhibitory concentrations (IC_{50}) of benzydamine on these cells at 48 h were 43.6, 38.2, 42.3, 30.4, 36.2, 39.8 and 91.0 μM, respectively (Fig. 1C, Fig. S1A). Subsequently, we used different doses of benzydamine to examine its effects on the anchorage-dependent growth of these cells. We found that benzydamine inhibited the anchorage-dependent growth of these ESCC cells, but did not significantly inhibit SHEE cells (Fig. 1D, Fig. S1B). We then verified the effect of benzydamine on the anchorage-independent growth of KYSE150 and KYSE450 cells using a soft agar assay. Our results demonstrated that benzydamine suppressed the anchorage-independent growth of ESCC cells in a dose-dependent manner (Fig. 1E). The results from plate clone formation assays also indicated that benzydamine-treated groups had fewer colony numbers than the control group in KYSE150 and KYSE450 cells (Fig. 1F).

Phosphoproteomic profiles of KYSE150 cells after benzydamine treatment

To explore the inhibitory mechanism of benzydamine on ESCC, we conducted phosphoproteomic analysis to comprehensively analyze the changes in the phosphorylation level of proteins of KYSE150 cells after benzydamine treatment [22]. The mass spectrometry proteomics data have been deposited to the ProteomeXchange Consortium via the iProX partner repository

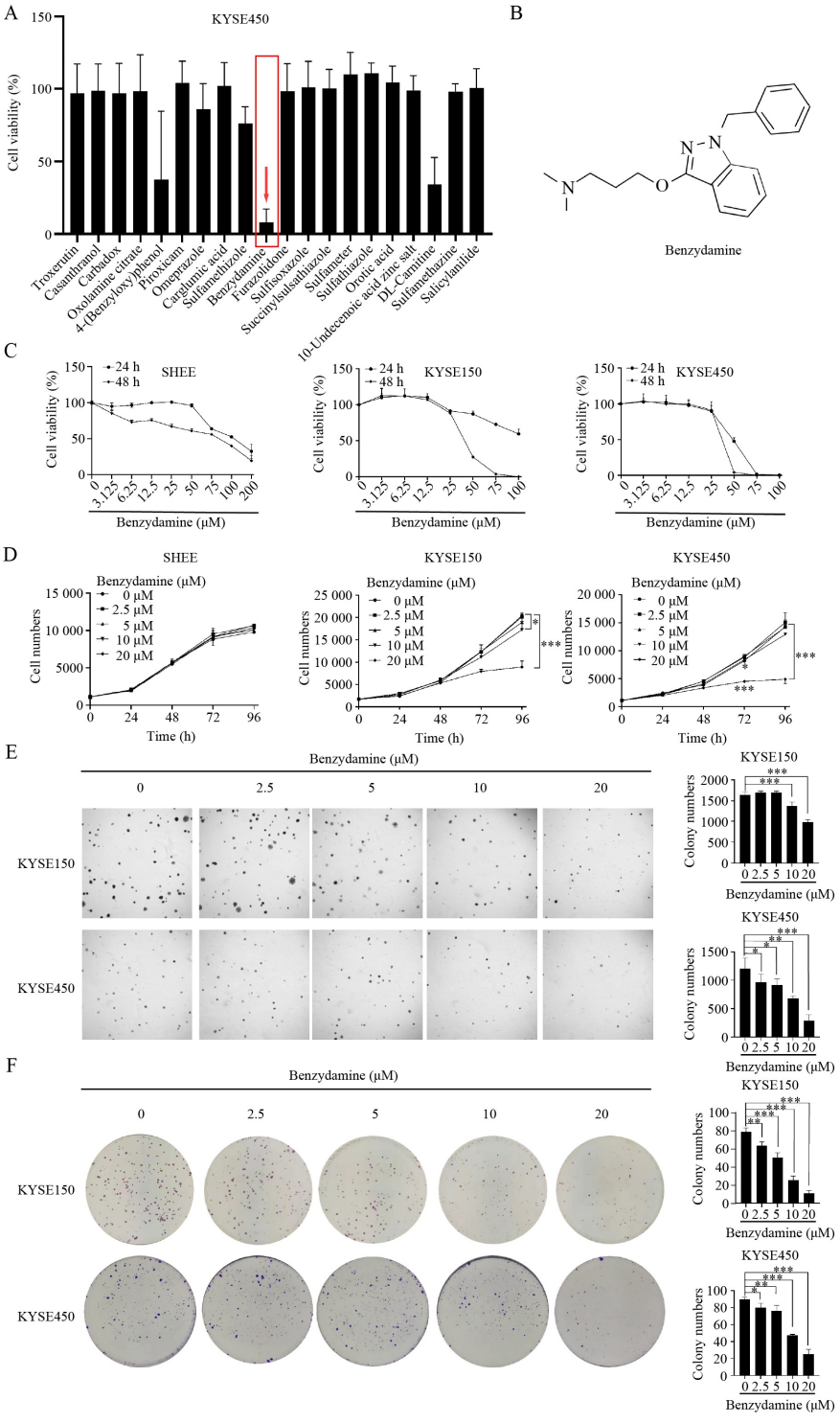

Fig. 1 Benzydamine suppressed the anchorage-dependent and -independent growth of ESCC cells. (A) Effect of 20 FDA-approved drugs (No. 1–20) on cell proliferation. KYSE450 cells were treated with drugs (50 μM) for 48 h and the cell survival rate was measured. (B) Chemical structure of benzydamine. (C) KYSE150, KYSE450, and SHEE cells treated with benzydamine for 24 and 48 h. Cell viability was measured using the IN Cell Analyzer 6000 software. (D) Effect of benzydamine on the proliferation of SHEE cells and ESCC cells for 24, 48, 72, and 96 h. (E) ESCC cells treated with benzydamine for 2 weeks. Colony numbers were counted using the IN Cell Analyzer 6000 and Image J software. Quantitative analysis was on the right panel. (F) Clone formation assay and quantitative analysis were conducted on KYSE150 and KYSE450 cells. Cells were treated with different concentrations of benzydamine and then stained with crystal violet dye. The data in (D–F) were derived from three independent experiments and are presented as mean ± SD. Asterisks (*, **, ***) indicated a significant decrease ($P < 0.05$, $P < 0.01$, $P < 0.001$, respectively) by one-way ANOVA followed by multiple-comparison tests. Similar results were obtained in three independent experiments.

[23] with the data set identifier PXD034404. Phosphorylation changes were analyzed following a precise standard (*t*-test *P*-value < 0.05, 1.5-fold change from baseline as the threshold). We identified a total of 3496 proteins, of which 2982 proteins were quantified (Fig. S2). Among the differentially expressed proteins, 159 proteins were upregulated, whereas 363 proteins were downregulated. We also identified a total of 14 069 phosphorylation sites, among which 8509 sites were quantified. Among these quantified phosphosites, 191 sites were upregulated, whereas 500 sites were downregulated in KYSE150 cells after treated with 20 μM benzydamine (Fig. 2A and 2B). Then, we mapped the quantified phosphosites to Kyoto Encyclopedia of Genes and Genomes (KEGG) pathway enrichment [24]. We observed that the top five downregulated signaling pathways included RNA transport, DNA replication, spliceosome, ferroptosis, and protein processing in the endoplasmic reticulum. The phosphoproteomic data suggested that multiple phosphorylation sites that essentially related with cancer-driver genes were downregulated in the DNA replication signaling pathway (Fig. 2C). Interestingly, we found that the MCM2 S41 was obviously downregulated in both the DNA replication and cell cycle signaling pathways (Fig. 2D). MCM2 S41 is known to participate in the initiation of DNA synthesis and is reportedly required for entry into the S phase and for cell division. Our results suggested that the phosphorylation of MCM2 S41, c-Myc S62 and Rb T826 were inhibited after benzydamine treatment (Fig. 2E). To explore the underlying mechanism of the anti-tumor effect of benzydamine, we performed kinase prediction and Swiss TargetPrediction to identify the upstream kinases. We observed that CDK2 was the most promising molecular target of benzydamine. Additionally, Spearman's correlation analysis of the expression of the CDK2 and MCM2 genes representing the CDK2/MCM2 signaling pathway also showed significant differences (P = 2.58e–14) (Fig. 2F).

Benzydamine induced G1/S phase arrest and inhibited the DNA replication pathway

Due to the role of CDK2 in cell cycle distribution, we further investigated the effect of benzydamine on cell cycle. We found benzydamine affected the cell cycle distribution in the KYSE150 and KYSE450 ESCC cell lines (Fig. 3A and 3B). Clearly, benzydamine caused a significant G1/S phase cell cycle arrest in KYSE150 and KYSE450 cells (P < 0.05). Additionally, immunofluorescent results suggested benzydamine decreased the phosphorylation of MCM2 S41 in KYSE150 and KYSE450 cells. Based on these results, we detected the phosphorylation levels of proteins involved in the transition from G1 to S phase during the cell cycle (Fig. 3C and 3D). We found that compared with the DMSO control, benzydamine reduced the phosphorylation of MCM2 S41, c-Myc S62 and Rb T826 in ESCC cells in a dose-dependent manner (Fig. 3E and 3F).

Benzydamine directly bound to CDK2 and inhibited CDK2 kinase activity

To investigate the target of benzydamine, we first analyzed phosphorylomics data after benzydamine treatment to obtain a list of active downregulated kinases (Table S1). We evaluated the list of benzydamine docking kinases using the Swiss TargetPrediction [16] and SwissDock [17] (Table S2). Through the comprehensive analysis of the two tables, we hypothesized that CDK2 might be the target of benzydamine in ESCC. To investigate the possible mechanism involved in the benzydamine-CDK2 interaction, we downloaded the CDK2 kinase domain (PDB: 1AQ1) and docked it with benzydamine following the protocols in the autodock software programs [25,26]. According to the docking model, we found that benzydamine formed a hydrogen bond with the 145th amino acid of CDK2, which was also known to be an ATP binding site affecting kinase activity. The 80th and 146th amino acids of CDK2 have intermolecular forces with benzydamine, which may also affect the binding of CDK2 to benzydamine. This data suggested that benzydamine competed with ATP for binding at the ATP binding site of CDK2 (Fig. 4A). To further verify this result, we performed a pull-down assay by conjugating benzydamine with Sepharose 4B beads. We found that the recombinant CDK2 protein bound with benzydamine-conjugated Sepharose 4B beads but not with Sepharose 4B beads alone (Fig. 4B). We then constructed mutant CDK2 (F80A, D145A, F146A, D145A and F146A) plasmids and ectopically expressed these mutants in 293F cells. Results of pull-down assays revealed that the D145A CDK2 mutant proteins bound to benzydamine were strong reduced compared to wild-type CDK2, indicating that 145th aspartic acid of CDK2 was essential for benzydamine binding (Fig. 4C). We further performed pull-down assays using KYSE150 and KYSE450 cell lysates, the results suggested that benzydamine could also bind to CDK2 (Fig. 4D). Interestingly, we also determined that the binding between benzydamine and CDK2 was ATP-competitive (Fig. 4E). And, sequence alignments of CDK2 phosphorylation domain among multiple species showed that 145th aspartic acid of CDK2 was highly evolutionarily conserved (Fig. S3). We also found that benzydamine inhibited the pan-serine phosphorylation of MCM2 and CDK2. The downregulation of CDK2 phosphorylation may be due to the inhibition of CDK2 autophosphorylation (Fig. 4F). Then, we performed an *in vitro* kinase assay using an active recombinant CDK2 protein and MCM2 as a

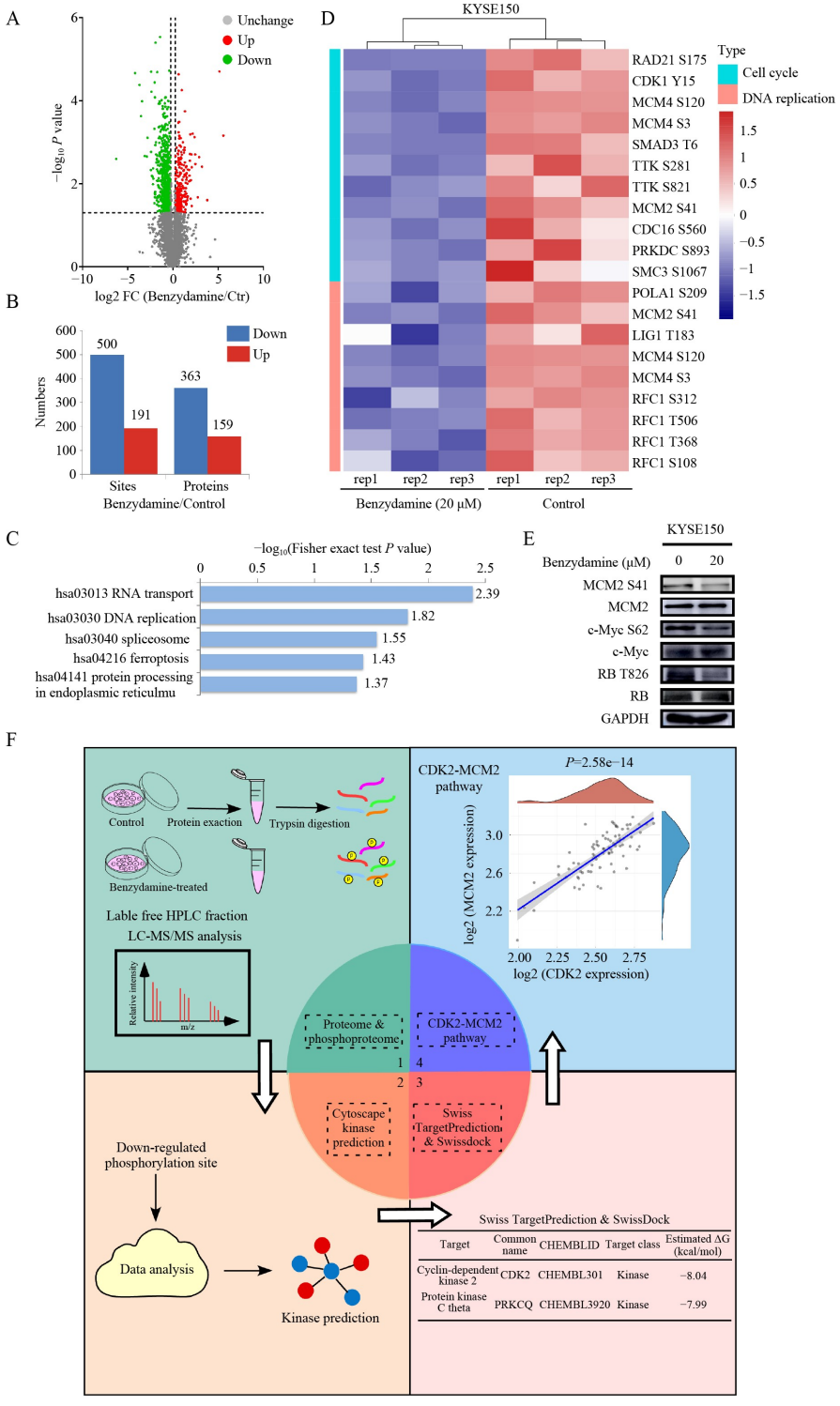

Fig. 2 Phosphoproteomic profiles of KYSE150 cells after benzydamine treatment. (A)Volcano plot of differentially-expressed phosphorylation proteins, blue dots represented downregulated sites, whereas red dots represented upregulated sites. (B) Quantification of differentially-expressed proteins. (C) KEGG enrichment of downregulated phosphorylation sites (top five pathways). (D) Significantly changed phosphorylation sites involved in DNA replication and cell cycle signaling pathways were shown in heatmap. (E) Phosphorylation and expression levels of proteins were assessed by Western blotting. KYSE150 cells were treated with or without benzydamine for 24 h. (F) The schematic for analysis of multi-omics data and prediction of upstream protein kinases. The LC-MS/MS search and database research were first constructed for the proteome and phosphoproteome analyses. Swiss TargetPrediction and SwissDock were subsequently employed to predict upstream kinases. Spearman's correlation analysis of the expression of CDK2 and MCM2 genes. Datasets used were comprised of mRNA-seq data from TCGA. Quantified protein and phosphorylation sites were subjected to the following criteria ($P < 0.05$, fold change > 1.5).

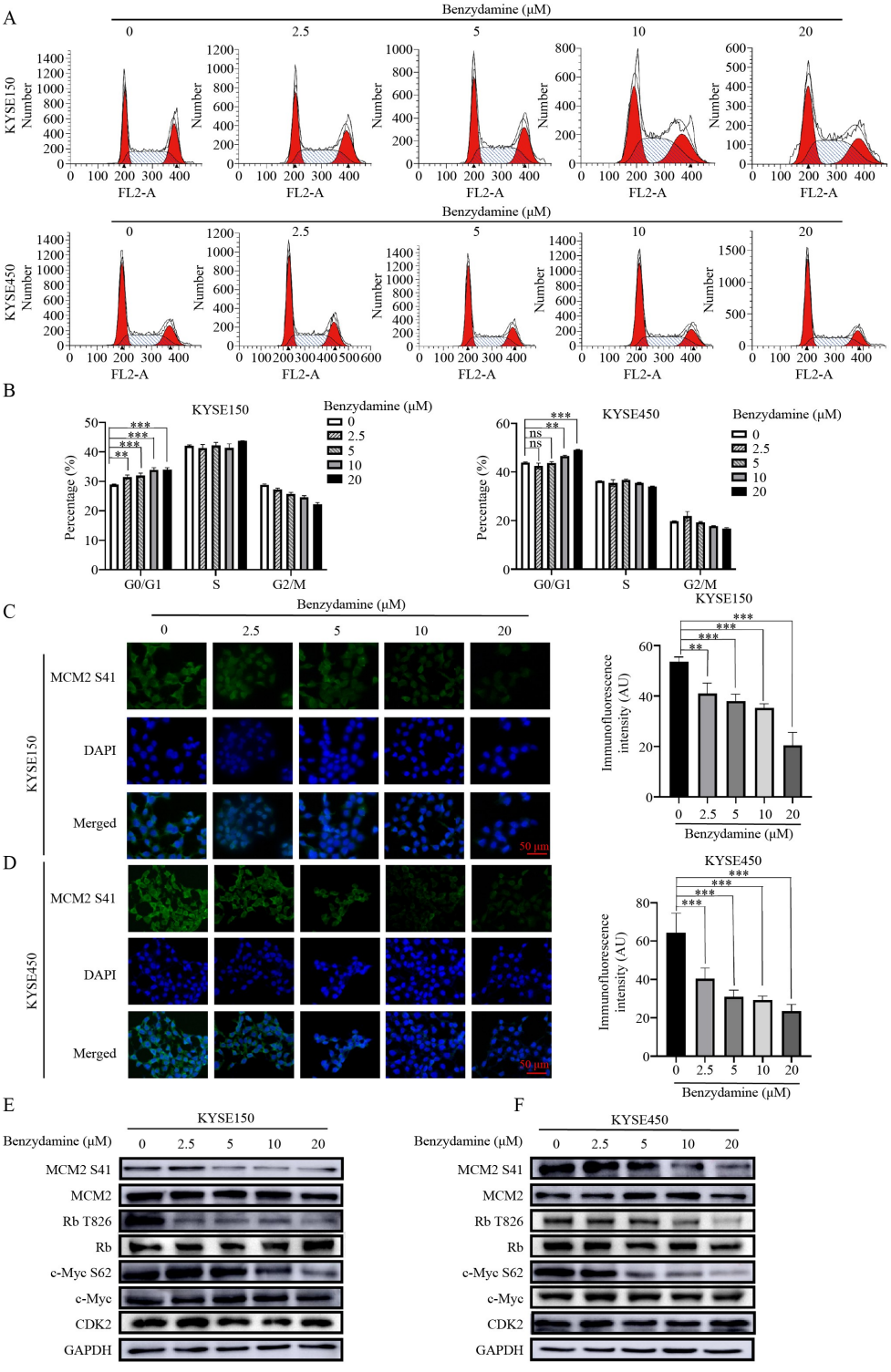

Fig. 3 Benzydamine induced G1/S phase arrest and inhibited the DNA replication pathway. (A, B) The effects of benzydamine on cell cycle phase were demonstrated using KYSE150 and KYSE450 ESCC cells. Cells were treated with various concentrations of benzydamine (0, 2.5, 5, 10, or 20 μM) and incubated for 24 h (KYSE150) or 48 h (KYSE450) for cell cycle analysis by flow cytometry. Bar graph displayed the distribution of cell cycle in KYSE150 and KYSE450 ESCC cells. (C, D) Immunofluorescence staining of KYSE150 and KYSE450 cells with or without benzydamine (2.5, 5, 10, or 20 μM) treatment for 24 h. Cells were stained with DAPI (blue) and MCM2 S41 (green). Scale bars, 50 μm. (E, F) KYSE150 and KYSE450 cells were with benzydamine (0, 2.5, 5, 10, or 20 μM) and incubated for 24 h. The protein levels of MCM2 S41, c-Myc S62 and Rb T826 after benzydamine treatment. For the data in (A–D), asterisks (**$P < 0.01$, ***$P < 0.001$) indicated a significant difference between control and benzydamine-treated KYSE150 and KYSE450 cells. Data were displayed as mean ± SD by one way ANOVA followed by multiple comparisons.

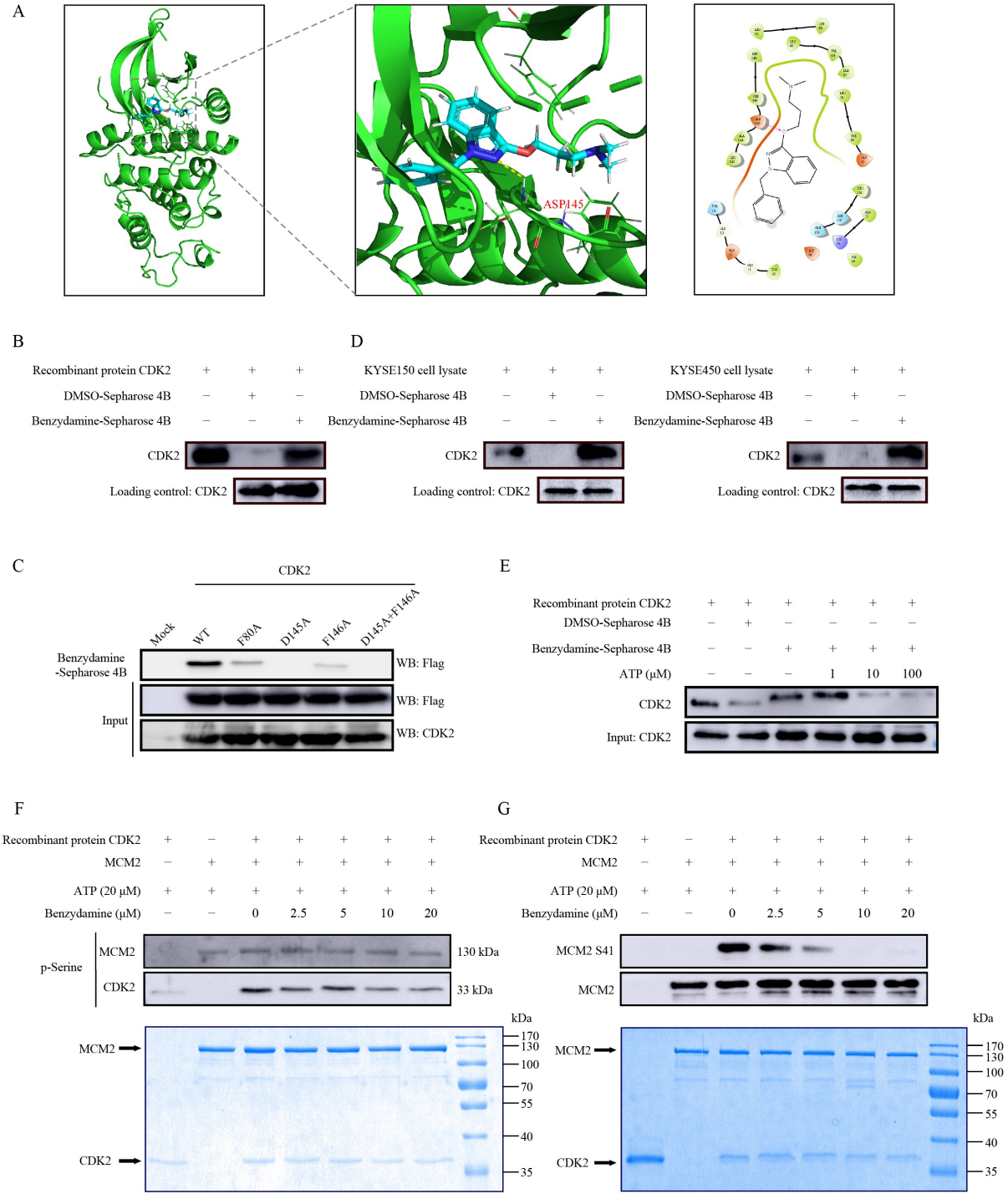

Fig. 4 Benzydamine directly bound to CDK2 and inhibited CDK2 kinase activity. (A) Model of benzydamine binding to CDK2 at the ATP binding site. (B, D) Active CDK2 (200 ng) and cell lysates of KYSE150 and KYSE450 were incubated with benzydamine-conjugated Sepharose 4B beads or with Sepharose 4B beads alone. Pull-down proteins were analyzed by Western blotting. (C) CDK2 (WT, F80A, D145A, F146A, D145A and D146A) proteins were incubated with benzydamine-conjugated Sepharose 4B beads or with Sepharose 4B beads alone. Pull-down proteins were analyzed by Western blotting. (E) The specificity of the binding between benzydamine and active CDK2 in the presence of ATP was evaluated. (F, G) Active CDK2 (500 ng) and various doses of benzydamine were incubated with MCM2 (1 μg) as a substrate at 30 °C for 30 min. The levels of p-Serine and MCM2 S41 were detected by Western blotting. CDK2 and MCM2 proteins were detected by Western blotting and Coomassie blue staining (the bottom picture).

substrate (Fig. S4). Our results suggested that the activity of CDK2 was strongly inhibited by benzydamine in a dose-dependent manner (Fig. 4G). Therefore, these results confirmed that benzydamine directly suppressed the activity of CDK2, resulting in inhibition of MCM2 phosphorylation on serine 41.

Knockdown of CDK2 decreased the sensitivity of ESCC cells to benzydamine

TCGA database analysis revealed that CDK2 was highly expressed in EC (Fig. 5A). To further investigate the function of CDK2 in ESCC tumor growth, we knocked down CDK2 in KYSE150 and KYSE450 cells with shCDK2. CDK2 knockdown reduced the phosphorylation of MCM2 S41, c-Myc S62 and Rb T826 in ESCC cells (Fig. 5B). We found that the CDK2 knockdown suppressed the proliferation of KYSE150 and KYSE450 cells (Fig. 5C). Moreover, we noticed that the colony formation ability of these cells was also inhibited after knocking down CDK2 (Fig. 5D and 5E). The effect of the CDK2 knockdown was also detected in cell cycle distribution (Fig. 5F and 5G). Our results suggested that CDK2 knockdown induced G1/S phase arrest in KYSE150 and KYSE450 cells. As benzydamine could bind to CDK2 protein and inhibited its kinase activity, we subsequently investigated the drug sensitivity of KYSE150 and KYSE450 cell lines to benzydamine after CDK2 knockdown. The results indicated that the drug sensitivity of KYSE150 and KYSE450 decreased after CDK2 knockdown (Fig. 5H).

Benzydamine suppressed patient-derived xenograft tumor growth *in vivo*

Next, we used the PDX models to evaluate the anti-tumor activity of benzydamine *in vivo*. Tumor tissues from patients were implanted into the backs of SCID mice. Mice were administered benzydamine (5 and 50 mg/kg) or vehicle. The results demonstrated that benzydamine treatment dramatically reduced the tumor volume in contrast to the vehicle group in cases EG20, LEG34, and LEG110 (Fig. 6A and 6B), while the average bodyweights were not obviously different between different groups (Fig. S5). The weights of the tumor tissues were measured, and the results indicated that tumor weights were reduced in mice treated with benzydamine (Fig. 6C). In addition, we also observed that benzydamine-treated mice did not exhibit an obvious loss of body weight compared with the vehicle-treated group. Then, we verified the findings of the phosphoproteomic profile at the tissue level using immunohistochemistry. Our results demonstrated that benzydamine decreased the levels of Ki67 and the phosphorylation level of MCM2 S41, but did not decrease CDK2 protein level, which was consistent with the results of cell experiments (Fig. 6D). In summary, these data indicated that benzydamine suppressed the growth of ESCC by inhibiting CDK2 pathway (Fig. 6E).

Discussion

The incidence and mortality of EC ranked seventh and sixth among all cancers in 2020 [27]. Thus, new drugs for EC targeted therapies are urgent needed. In this study, we showed that benzydamine significantly inhibited the proliferation and colony formation of ESCC cells *in vitro*, as well as the tumor growth of ESCC *in vivo* (Figs. 1 and 6). Benzydamine is a nonsteroidal anti-inflammatory drug that exerts anti-inflammatory effects by inhibiting COX-2 [28,29], and has been used to prevent postoperative sore throat [30], treat oral mucositis, and relieve pain in cancer patients receiving chemotherapy or radiotherapy [31]. Beyond its original use, this is the first study to establish the anti-tumor activity of benzydamine in ESCC. Since benzydamine is commonly used for postoperative analgesia in patients with upper gastrointestinal cancer, we believe that benzydamine has a good application prospect in patients with ESCC.

CDK2 belongs to the family of cyclin-dependent kinase complexes and plays a key role in the cell cycle [32]. Moreover, CDK2 phosphorylates MCM2, Rb, and c-Myc. During the G1 to S transition, cyclin E-CDK2 was found to phosphorylate MCM2 at Ser 41 to initiate DNA synthesis [33,34]. Meanwhile, this complex has also been reported to catalyze the hyper-phosphorylation of Rb at Thr 826, resulting in the promotion of tumor growth [35]. Additionally, cyclin E-CDK2 is known to phosphorylate c-Myc at Ser 62 and the phosphorylation can increase the biological activity of Myc, regulating cell cycle and tumor initiation [36,37]. Here, we found that benzydamine induced a G1/S arrest in ESCC cells in a dose-dependent manner by inhibiting the activity of CDK2 (Fig. 3). Benzydamine decreased the phosphorylation of MCM2 S41, RB T826, and c-Myc S62 by binding to CDK2 and inhibiting its activity, which has been critically related to tumor growth (Fig. 3E). Through molecular docking and experiments, we confirmed that benzydamine mainly bound to D145 of CDK2 and occupied the ATP binding site, thereby inhibiting CDK2 kinase activity (Fig. 4B–4E). Furthermore, we found that knocking down CDK2 restrained the growth and colony formation of ESCC cells. Importantly, knocking down CDK2 reduced its sensitivity to benzydamine treatment in ESCC cells (Fig. 5). Therefore, we confirmed that CDK2 is a target of benzydamine in ESCC cells.

PDX models provide a series of advantages over human cell line xenograft models for the evaluation of preclinical

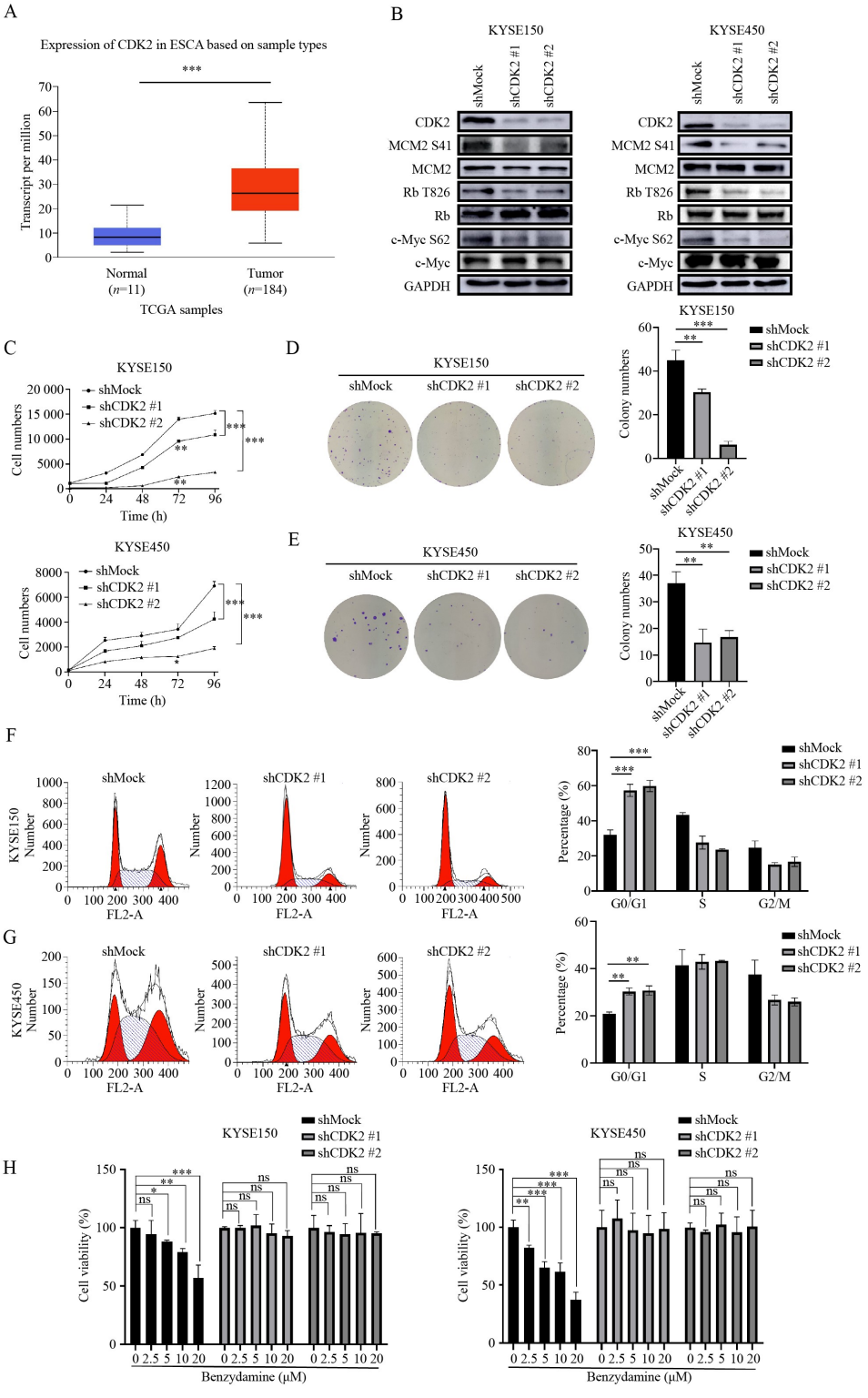

Fig. 5 Knockdown of CDK2 decreased the sensitivity of ESCC cells to benzydamine. (A) CDK2 was highly expressed in EC tumor tissues compared with normal tissues in TCGA database ($P = 1.764 \times 10^{-7}$). (B) The levels of MCM2 S41, c-Myc S62 and Rb T826 after CDK2 knockdown in KYSE150 and KYSE450 cells. (C–E) Knockdown CDK2 in KYSE150 and KYSE450 cells reduced the proliferation and colony formation ability of ESCC cells. Proliferation assay (C), plate cloning assay (D, E). (F, G) Knockdown CDK2 in KYSE150 and KYSE450 cells induced G1/S phase arrest. (H) Proliferation of KYSE150 and KYSE450 cells transfected with shMock or shCDK2, with or without treatment with various doses of benzydamine (0, 2.5, 5, 10, or 20 μM). Cell numbers were measured using the IN Cell Analyzer 6000 software. For (C–H), data were shown as the mean ± SD of triplicate values obtained from three independent experiments. Asterisks (*, **, ***) indicated a significant decrease ($P < 0.05$, $P < 0.01$, $P < 0.001$, respectively) by one-way ANOVA followed by multiple-comparison tests.

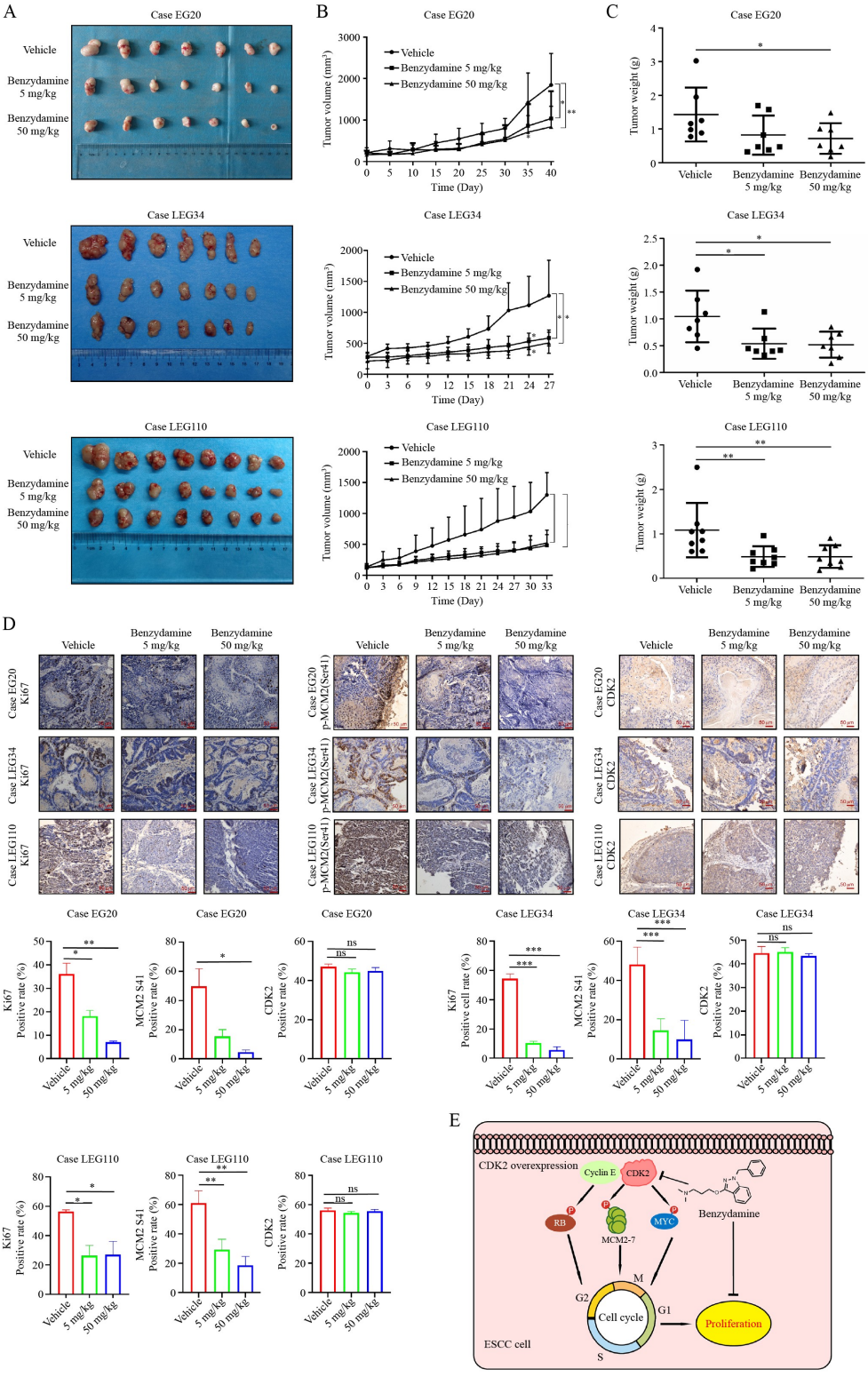

Fig. 6 Benzydamine suppressed patient-derived xenograft tumor growth *in vivo*. (A) Tumor images in different groups of EG20, LEG34 and LEG110 cases after sacrifice. (B) The changes of average tumor volumes in different group of EG20, LEG34 and LEG110 cases after benzydamine treatment. (C) Tumor weight analysis in different groups of EG20, LEG34 and LEG110 cases after benzydamine treatment. (D) Immunohistochemistry analysis of Ki67, MCM2 S41 and CDK2 in cases EG20, LEG34, and LEG110 after benzydamine treatment. The positive cell rates were evaluated by Histo Quest-shortcut software. All data were shown as the mean ± SD. (E) Schematic illustrating the anti-tumor activity of benzydamine. Asterisks (*, **, ***) indicated a significant decrease ($P < 0.05$, $P < 0.01$, $P < 0.001$, respectively) by one-way ANOVA followed by multiple-comparison tests.

therapies and prediction of responsiveness to anti-cancer treatments because they retain more genetic characteristics of the tumor specimens of patients [38–40]. In this study, we found that benzydamine suppressed tumor growth of ESCC and PDX tumors in mice by attenuating the phosphorylation of MCM2 at serine 41. Additionally, the expression of Ki67, a proliferation marker [41], was also reduced in tumor tissues after benzydamine treatment (Fig. 6). These findings indicated that benzydamine could suppress the tumor growth of ESCC *in vivo* by targeting the CDK2 signaling pathway.

Conclusions

In this study, we identify that benzydamine, a NSAID, has the anti-tumor effect against ESCC. Our work highlights benzydamine suppresses the growth of esophageal squamous cell carcinoma growth *in vitro* and *in vivo* by targeting CDK2 and inducing cell cycle arrest (Fig. 6E).

Acknowledgments

This work was supported by the National Natural Science Foundations of China (No. 81872335), the National Natural Science Youth Foundation (No. 81902486), the Natural Science Foundation of Henan (No. 161100510300), the Central Plains Science and Technology Innovation Leading Talents (No. 224200510015), the Science and Technology Project of Henan Province (No. 212102310187).

Compliance with ethics guidelines

Yubing Zhou, Xinyu He, Yanan Jiang, Zitong Wang, Yin Yu, Wenjie Wu, Chenyang Zhang, Jincheng Li, Yaping Guo, Xinhuan Chen, Zhicai Liu, Jimin Zhao, Kangdong Liu and Zigang Dong declare no competing interests. This study was approved by the Research Ethics Committee of Zhengzhou University. Written informed consent was provided by all patients for the use of the tissue samples.

Electronic Supplementary Material Supplementary material is available in the online version of this article at https://doi.org/10.1007/s11684-022-0956-8 and is accessible for authorized users.

References

1. Yuan Z, Wang X, Geng X, Li Y, Mu J, Tan F, Xue Q, Gao S, He J. Liquid biopsy for esophageal cancer: is detection of circulating cell-free DNA as a biomarker feasible? Cancer Commun (Lond) 2021; 41(1): 3–15
2. Abnet CC, Arnold M, Wei WQ. Epidemiology of esophageal squamous cell carcinoma. Gastroenterology 2018; 154(2): 360–373
3. Yang YM, Hong P, Xu WW, He QY, Li B. Advances in targeted therapy for esophageal cancer. Signal Transduct Target Ther 2020; 5(1): 229
4. di Pietro M, Canto MI, Fitzgerald RC. Endoscopic management of early adenocarcinoma and squamous cell carcinoma of the esophagus: screening, diagnosis, and therapy. Gastroenterology 2018; 154(2): 421–436
5. Reichenbach ZW, Murray MG, Saxena R, Farkas D, Karassik EG, Klochkova A, Patel K, Tice C, Hall TM, Gang J, Parkman HP, Ward SJ, Tétreault MP, Whelan KA. Clinical and translational advances in esophageal squamous cell carcinoma. Adv Cancer Res 2019; 144: 95–135
6. Surh YJ. Cancer chemoprevention with dietary phytochemicals. Nat Rev Cancer 2003; 3(10): 768–780
7. Desai P, Thumma NJ, Wagh PR, Zhan S, Ann D, Wang J, Prabhu S. Cancer chemoprevention using nanotechnology-based approaches. Front Pharmacol 2020; 11: 323
8. Ranjan A, Ramachandran S, Gupta N, Kaushik I, Wright S, Srivastava S, Das H, Srivastava S, Prasad S, Srivastava SK. Role of phytochemicals in cancer prevention. Int J Mol Sci 2019; 20(20): 4981
9. Chen CY, Kuo CJ, Lee YW, Lam F, Tam KW. Benzydamine hydrochloride on postoperative sore throat: a meta-analysis of randomized controlled trials. Can J Anaesth 2014; 61(3): 220–228
10. Faber EB, Wang N, Georg GI. Review of rationale and progress toward targeting cyclin-dependent kinase 2 (CDK2) for male contraception†. Biol Reprod 2020; 103(2): 357–367
11. Fagundes R, Teixeira LK. Cyclin E/CDK2: DNA replication, replication stress and genomic instability. Front Cell Dev Biol 2021; 9: 774845
12. Tetsu O, McCormick F. Proliferation of cancer cells despite CDK2 inhibition. Cancer Cell 2003; 3(3): 233–245
13. Au-Yeung G, Lang F, Azar WJ, Mitchell C, Jarman KE, Lackovic K, Aziz D, Cullinane C, Pearson RB, Mileshkin L, Rischin D, Karst AM, Drapkin R, Etemadmoghadam D, Bowtell DDL. Selective targeting of cyclin E1-amplified high-grade serous ovarian cancer by cyclin-dependent kinase 2 and AKT inhibition. Clin Cancer Res 2017; 23(7): 1862–1874
14. Tadesse S, Anshabo AT, Portman N, Lim E, Tilley W, Caldon CE, Wang S. Targeting CDK2 in cancer: challenges and opportunities for therapy. Drug Discov Today 2020; 25(2): 406–413
15. Tadesse S, Caldon EC, Tilley W, Wang S. Cyclin-dependent kinase 2 inhibitors in cancer therapy: an update. J Med Chem 2019; 62(9): 4233–4251
16. Gfeller D, Grosdidier A, Wirth M, Daina A, Michielin O, Zoete V. SwissTargetPrediction: a web server for target prediction of bioactive small molecules. Nucleic Acids Res 2014; 42: W32–W38
17. Grosdidier A, Zoete V, Michielin O. SwissDock, a protein-small molecule docking web service based on EADock DSS. Nucleic Acids Res 2011; 39: W270–W277
18. Wang Z, Jensen MA, Zenklusen JC. A practical guide to The Cancer Genome Atlas (TCGA). Methods Mol Biol 2016; 1418: 111–141
19. Hu Y, Liu F, Jia X, Wang P, Gu T, Liu H, Liu T, Wei H, Chen H, Zhao J, Yang R, Chen Y, Dong Z, Liu K. Periplogenin suppresses the growth of esophageal squamous cell carcinoma *in vitro* and *in vivo* by targeting STAT3. Oncogene 2021; 40(23): 3942–3958
20. Jiang Y, Wu Q, Yang X, Zhao J, Jin Y, Li K, Ma Y, Chen X, Tian F, Zhao S, Xu J, Lu J, Yin X, Liu K, Dong Z. A method for

establishing a patient-derived xenograft model to explore new therapeutic strategies for esophageal squamous cell carcinoma. Oncol Rep 2016; 35(2): 785–792
21. Jin G, Yan M, Liu K, Yao K, Chen H, Zhang C, Yi Y, Reddy K, Gorja DR, Laster KV, Guo Z, Dong Z. Discovery of a novel dual-target inhibitor against RSK1 and MSK2 to suppress growth of human colon cancer. Oncogene 2020; 39(43): 6733–6746
22. Sürmen MG, Sürmen S, Ali A, Musharraf SG, Emekli N. Phosphoproteomic strategies in cancer research: a minireview. Analyst (Lond) 2020; 145(22): 7125–7149
23. Ma J, Chen T, Wu S, Yang C, Bai M, Shu K, Li K, Zhang G, Jin Z, He F, Hermjakob H, Zhu Y. iProX: an integrated proteome resource. Nucleic Acids Res 2019; 47(D1): D1211–D1217
24. Kanehisa M, Furumichi M, Tanabe M, Sato Y, Morishima K. KEGG: new perspectives on genomes, pathways, diseases and drugs. Nucleic Acids Res 2017; 45(D1): D353–D361
25. Burley SK, Berman HM, Kleywegt GJ, Markley JL, Nakamura H, Velankar S. Protein Data Bank (PDB): the single global macromolecular structure archive. Methods Mol Biol 2017; 1607: 627–641
26. Trott O, Olson AJ. AutoDock Vina: improving the speed and accuracy of docking with a new scoring function, efficient optimization, and multithreading. J Comput Chem 2010; 31(2): 455–461
27. Sung H, Ferlay J, Siegel RL, Laversanne M, Soerjomataram I, Jemal A, Bray F. Global cancer statistics 2020: GLOBOCAN estimates of incidence and mortality worldwide for 36 cancers in 185 countries. CA Cancer J Clin 2021; 71(3): 209–249
28. Cioli V, Corradino C, Scorza Barcellona P. Review of pharmacological data on benzydamine. Int J Tissue React 1985; 7(3): 205–213
29. Quane PA, Graham GG, Ziegler JB. Pharmacology of benzydamine. Inflammopharmacology 1998; 6(2): 95–107
30. Singh NP, Makkar JK, Wourms V, Singh PM. Topical benzydamine for preventing postoperative sore throat. Anaesthesia 2018; 73(10): 1297
31. Worthington H V. , Clarkson JE, Bryan G, Furness S, Glenny AM, Littlewood A, McCabe MG, Meyer S, Khalid T, Riley P. Interventions for preventing oral mucositis for patients with cancer receiving treatment. Cochrane database Syst Rev 2011; 2011(4): CD000978
32. Golsteyn RM. Cdk1 and Cdk2 complexes (cyclin dependent kinases) in apoptosis: a role beyond the cell cycle. Cancer Lett 2005; 217(2): 129–138
33. Tsuji T, Ficarro SB, Jiang W. Essential role of phosphorylation of MCM2 by Cdc7/Dbf4 in the initiation of DNA replication in mammalian cells. Mol Biol Cell 2006; 17(10): 4459–4472
34. Poon RYC. Cell cycle control: a system of interlinking oscillators. Methods Mol Biol 2016; 1342: 3–19
35. Harbour JW, Luo RX, Santi AD, Postigo AA, Dean DC. Cdk phosphorylation triggers sequential intramolecular interactions that progressively block Rb functions as cells move through G1. Cell 1999; 98(6): 859–869
36. Hydbring P, Larsson LG. Tipping the balance: Cdk2 enables Myc to suppress senescence. Cancer Res 2010; 70(17): 6687–6691
37. Hydbring P, Castell A, Larsson LG. MYC modulation around the CDK2/p27/SKP2 axis. Genes (Basel) 2017; 8(7): 174
38. Garcia PL, Miller AL, Yoon KJ. Patient-derived xenograft models of pancreatic cancer: overview and comparison with other types of models. Cancers (Basel) 2020; 12(5): 1327
39. Klöß S, Dehmel S, Braun A, Parnham MJ, Köhl U, Schiffmann S. From cancer to immune-mediated diseases and tolerance induction: lessons learned from immune oncology and classical anti-cancer treatment. Front Immunol 2020; 11: 1423
40. Hidalgo M, Amant F, Biankin AV, Budinská E, Byrne AT, Caldas C, Clarke RB, de Jong S, Jonkers J, Mælandsmo GM, Roman-Roman S, Seoane J, Trusolino L, Villanueva A. Patient-derived xenograft models: an emerging platform for translational cancer research. Cancer Discov 2014; 4(9): 998–1013
41. Nielsen TO, Leung SCY, Rimm DL, Dodson A, Acs B, Badve S, Denkert C, Ellis MJ, Fineberg S, Flowers M, Kreipe HH, Laenkholm AV, Pan H, Penault-Llorca FM, Polley MY, Salgado R, Smith IE, Sugie T, Bartlett JMS, McShane LM, Dowsett M, Hayes DF. Assessment of Ki67 in breast cancer: updated recommendations from the international Ki67 in breast cancer working group. J Natl Cancer Inst 2021; 113(7): 808–819